PHYSICAL REVIEW A **81**, 051802(R) (2010)

Revealing molecular structure and dynamics through high-order harmonic generation driven by mid-IR fields

R. Torres,[1] T. Siegel,[1] L. Brugnera,[1] I. Procino,[2] Jonathan G. Underwood,[2,3] C. Altucci,[4] R. Velotta,[4] E. Springate,[3] C. Froud,[3] I. C. E. Turcu,[3] S. Patchkovskii,[5] M. Yu. Ivanov,[1] O. Smirnova,[6] and J. P. Marangos[1]

[1]*Blackett Laboratory, Imperial College London, Prince Consort Road, London SW7 2BW, United Kingdom*

[2]*Department of Physics and Astronomy, University College London, Gower Street, London WC1E 6BT, United Kingdom*

[3]*Central Laser Facility, Science and Technology Facilities Council, Rutherford Appleton Laboratory, Chilton, Didcot, Oxon OX11 0QX, United Kingdom*

[4]*Consorzio Nazionale Interuniversitario per le Scienze Fisiche della Materia and Dipartimento di Scienze Fisiche, Università di Napoli "Federico II," Naples, Italy*

[5]*Steacie Institute for Molecular Sciences, National Research Council of Canada, 100 Sussex Drive, Ottawa, Ontario K1A 0R6, Canada*

[6]*Max-Born-Institute, 2a Max-Born-Strasse, Berlin D-12489, Germany*

(Received 10 November 2009; published 18 May 2010)

High-order harmonic generation (HHG) from molecules produces spectra that are modulated by interferences that encode both the static structure and the electron dynamics initiated by interaction with the laser field. Using a midinfrared (mid-IR) laser at 1300 nm, we are able to study the region of the harmonic spectrum containing such interferences in CO_2 over a wide range of intensities. This allows for isolation and characterization of interference minima arising due to subcycle electronic dynamics triggered by the laser field, which had previously been identified but not systematically separated. Our experimental and theoretical results demonstrate important steps toward combining attosecond temporal and angstrom-scale spatial resolution in molecular HHG imaging.

DOI: 10.1103/PhysRevA.81.051802 PACS number(s): 42.65.Ky, 42.65.Re

High-order harmonic generation (HHG) spectroscopy is a new tool for measuring molecular structure [1–5] and dynamics [6–10], including subfemtosecond rearrangements of nuclei [6,7] and electrons [9,10]. This technique relies upon measuring the spectrum of coherent radiation emitted by molecules aligned in space when interacting with intense laser fields. To fully exploit HHG spectroscopy, one has to be able to (1) extend the method to a wide range of molecules and harmonic photon energies and (2) distinguish and characterize structural and dynamic effects in the measurement. The dominant features in the HHG spectrum are characteristic of ionization from the highest occupied molecular orbital (HOMO). However, involvement of lower lying orbitals in the HHG process [8–11] gives rise to attosecond multi-electron dynamics that are also manifested in the spectra [9,10]. We show that recording a broad range of harmonics for different laser intensities provides a method for time-resolved measurements of attosecond multielectron dynamics, identifying and separating contributions of electronic structure and dynamics.

Theory [1,12] and experiments [3,4,13,14] have established that HHG spectra from spatially aligned molecules encode the structure and symmetries of molecular orbitals. The key component of imaging these structures is the control of the angle between the molecular axes and the polarization of the driving laser field which determines the motion of the recolliding electron. This control is achieved through nonadiabatic molecular alignment with a preceding laser pulse [15]. The well-defined mapping of the delay between ionization and recombination onto the energy of the emitted harmonic allows one to obtain dynamical information on ultrafast structural rearrangements with ~100-as resolution [6–10].

In order to record structural features arising from typical internuclear distances (in the range of 1–2 Å), a harmonic spectrum reaching up to ~70 eV is required. By using a Ti:sapphire laser at 800 nm, the laser system generally employed in HHG, such harmonic spectra demand laser intensities in excess of 3×10^{14} W cm^{-2}, well above the ionization saturation intensity of most molecules. This requirement limits the capabilities of intensity-dependent studies, such as [9], because the full structural contribution to the harmonic spectrum cannot be probed at lower intensities. The extension of the range of intensities that can be used in the study of the critical portion of the harmonic spectrum (from 30 to 70 eV in CO_2) is the key advantage of using a laser of longer wavelength. It permits the spectrum to be studied in the plateau region over a wide range of laser intensities, $(1.0–2.0) \times 10^{14}$ W cm^{-2}, which allows the efficient reading of both structural and dynamic interference features.

The observation of a distinct minimum in the harmonic spectra from aligned samples of CO_2 was initially interpreted as evidence of solely structure-related two-center interference arising from a single-electron response from the HOMO (referred to as *structural minimum* in what follows), which would be intensity independent [3,4,16,17]. Recent experiments and advances in theory have shown that the physics of strong field interactions with molecules is more complicated than initially thought [8–11,16–19]. For example, the minimum in the harmonic spectrum from aligned CO_2 has been shown to depend on the laser intensity, shifting by ~20 eV for laser intensities $(0.5–2.0) \times 10^{14}$ W cm^{-2} [9]. In this earlier work, at 800 nm it was not possible to observe the structural interference as the cutoff position in the spectra was at energies less than the structural minimum.

It has been shown [9,10,19] that ionization via optical tunneling can populate several ionic states, creating a multielectron wave packet visualized as the motion of the hole left by ionization. This multielectron wave packet evolves on an attosecond time scale during the recollision process. A minimum in the harmonic spectra can result not only from molecular

structure but also from the motion of the hole, manifested as a time-dependent interference between the contributions of the HHG channels associated with different ionic states [9,10,19]. That is, for specific recollision times, the contributions from different ionic states will interfere destructively, giving rise to a reduction in the intensity of the harmonic corresponding to that recollision time [9]. Following [9,10,19], we refer to this phenomenon as *dynamical interference*. For measurements at 800 nm, this interpretation has matched the observed intensity dependence of the position of the minimum in CO_2 [9]. The combination of structural and dynamical information in the harmonic spectra opens new avenues for imaging but requires the ability to distinguish the two contributions. We show how a structure-related minimum in the harmonic spectrum from the HOMO reveals contributions from other molecular orbitals, demonstrating the dynamical information within the window provided by the structural minimum. Thus, the attosecond temporal resolution encoded in HHG spectra is ideally suited for following multielectron dynamics.

Harmonics generated with a 1300-nm pulse were found to offer a good compromise between cutoff energy and efficiency. For a given laser intensity at this wavelength, the ponderomotive energy, and hence the width and the maximal energy of the harmonic spectrum, is increased by a factor of 2.6 relative to 800 nm. A 1-kHz Ti:sapphire Chirped Pulse Amplification (CPA) laser system at 800 nm was used to pump an optical parametric amplifier delivering 1300-nm pulses with energies up to 1 mJ and 40-fs pulse duration for harmonic generation. Additional pulses from the 800-nm pump with field polarized at a variable angle Θ with respect to the mid-IR field were employed for impulsive molecular alignment [15]. The 1300- and 800-nm beams were sent collinearly into the interaction chamber, where a 30-cm-focal-length lens focused the two beams onto a continuous flow gas jet. The temperature of the gas in the interaction region was estimated as ~90 K, and the degree of molecular alignment was $\cos^2\theta \sim 0.6$. The gas jet was placed after the laser focus in order to select the short trajectory harmonics [20]. This selection, confirmed by the on-axis spatial distribution of the harmonic signal, is essential for the unambiguous mapping of electron excursion times onto photon energies. The interaction region was only 200 μm long, and the intensities were typically 10^{14} W cm^{-2} for the 1300-nm pulses and 5×10^{13} W cm^{-2} for the 800-nm pulse. A thin sample, significantly shorter than the coherence length, was deliberately employed to minimize the phase matching effects. Furthermore, both the phase mismatch and the absorption of harmonics in the medium vary smoothly with the wavelength [21]. The Gouy phase is approximately constant across the interaction region, and the change in index of refraction induced by the aligned sample is negligible. The energy of the 1300-nm pulses was varied using wedges to incrementally attenuate the beam without modifying significantly the pulse duration or beam profile. For larger attenuations, a variable aperture was used. The energy measurements were correlated with focal spot measurements to establish the intensity, and the relative changes of intensity were corroborated by the measured changes of harmonic cutoff position. The harmonic emission was analyzed in a flat-field Extreme Ultraviolet (XUV) spectrometer and detected on a microchannel plate. Each spectrum typically was averaged over 10^4 laser shots.

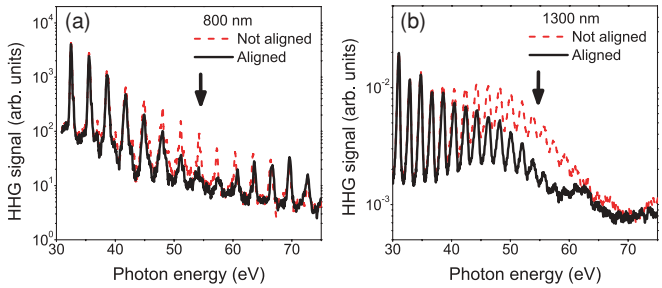

FIG. 1. (Color online) Comparison of HHG spectra in unaligned (dashed red) and aligned at $\Theta = 0^\circ$ (solid black) samples of CO_2: (a) with 800-nm drive field at 3.5×10^{14} W cm^{-2} (from Ref. [4]); (b) with 1300-nm drive field at 1.0×10^{14} W cm^{-2}. The arrows mark the position of the minima.

Harmonic spectra with photon energies reaching beyond 60 eV were detected in CO_2 for a wide range of laser intensities $(0.7–1.7) \times 10^{14}$ W cm^{-2}. The effect of molecular axis alignment was observed as a modulation in the harmonic signal when the delay between the driving and the aligning pulses was varied [22]. This delay was subsequently set to the time of maximum alignment, and the polarization of the aligning field was varied with a half-wave plate, allowing us to measure the harmonic signal as a function of the alignment of the molecular ensemble relative to the polarization of the driving field.

A harmonic spectrum from CO_2 previously obtained at 800 nm by Vozzi *et al.* [4] with intensity 3.5×10^{14} W cm^{-2} had the cutoff at around 80 eV [Fig. 1(a)]. With the 1300-nm field, we obtained a spectrum extending beyond 70 eV using an intensity of only 1.0×10^{14} W cm^{-2}, less than one-third of that employed in the 800-nm case [Fig. 1(b)]. Comparing the spectrum from an unaligned sample (red curves) with a sample aligned at $\Theta = 0^\circ$ (black curves), we see that the aligned sample shows a deep minimum. The HOMO in these molecules has a characteristic two-center structure. Contributions to the recombination amplitude from the two centers can interfere constructively or destructively [1] if the returning electrons have a de Broglie wavelength that satisfies the condition $\frac{n}{2}\lambda_{\mathrm{deB}} = R\cos\theta$, where n is an integer, R is the internuclear distance, and θ is the angle between the internuclear axis and the laser polarization vector. For the antibonding π_g HOMO of CO_2, the first destructive interference, or structural minimum, is expected for $n = 2$. In CO_2, with a separation between the oxygen atoms of 2.2 Å, the observed dip in the harmonic spectrum for $\Theta = 0^\circ$ is centered at 55 eV. Given that at $\Theta = 0^\circ$ the most probable angle between the field and the molecular axis for typical alignment conditions is $\theta \approx 30^\circ$ [23], our data are compatible with destructive structural interference, expected around 52 eV if one neglects acceleration of the electron by the core. In an accurate calculation, using the strong-field eikonal-Volkov approximation [24], including electron-exchange corrections and the dominance of ionization around ~45°, the interference minimum is found at 60 eV [19].

The minimum could also result from attosecond hole dynamics in the ion [9], manifested via destructive interference of different harmonic-generation pathways via different ionic states, here $\tilde{\mathbf{X}}\,^2\Pi_g$ and $\tilde{\mathbf{B}}\,^2\Sigma_u^+$ (referred to as X and B channels

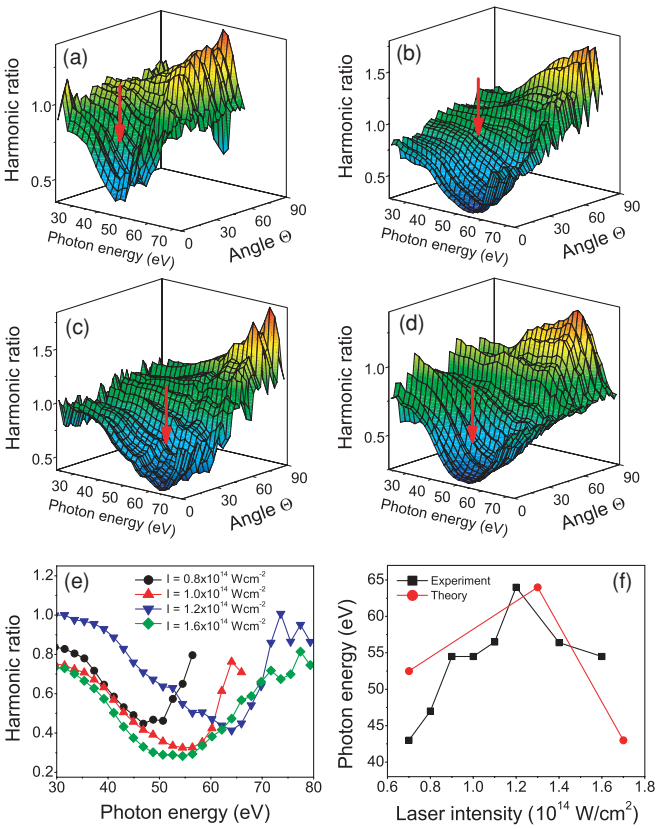

FIG. 2. (Color online) (a)–(d) HHG ratios between aligned and unaligned CO_2 as a function of photon energy and aligning angle for driving intensities: (0.8, 1.0, 1.2, and 1.6) $\times 10^{14}$ W cm^{-2} respectively. (e) Cut of figures (a)–(d) along $\Theta = 0°$. (f) Position of the interference minimum as a function of laser intensity.

later. One might expect this dynamical minimum to appear at the same time delay between ionization and recombination and hence at different photon energies for the two wavelengths (800 nm and 1300 nm). However, this simple picture is not always correct [10]. We observe that the minimum occurs at energies around 55 eV for both wavelengths. This result highlights the importance of the structural minimum in the recombination cross section, further emphasized through the results of our calculation.

Scans of the harmonic signal as a function of the angle Θ between the polarizations of the harmonic-generating (driving) field and the aligning field were taken in aligned samples of CO_2 at different intensities of the driving field [Figs. 2(a)–2(d)]. The signal recorded from the aligned ensemble is normalized against the unaligned case [25]. This normalization partially cancels other possible contributions to the structure of the HHG spectrum.

Systematic measurements of the intensity dependence of the minimum in CO_2 reveal a surprising result [Figs. 2(e) and 2(f)]. The minimum appears around 50 eV for the lowest intensities used (0.8×10^{14} W cm^{-2}) and increases to 65 eV at 1.2×10^{14} W cm^{-2} before returning to 55 eV upon further increase of intensity to 1.6×10^{14} W cm^{-2}. Such nonmonotonic intensity dependence of the minimum suggests interplay of structural and dynamical features in the harmonic spectrum.

The contribution of electronically excited states of the ion (i.e., from ionization of lower orbitals than the HOMO in the Hartree-Fock picture) to HHG is generally weaker than that of the HOMO. In CO_2, population of the ground state of the ion $\tilde{\mathbf{X}}\,^2\Pi_g$ (X channel) can be thought of as ionization from the HOMO. Similarly, population of the first excited state of CO_2^+, $\tilde{\mathbf{A}}\,^2\Pi_u$, corresponds to ionization from the HOMO-1 (A channel). The HOMO-1 has a nodal plane along the molecular axis, and the contribution of the A channel at small alignment angles is negligible. The HOMO-2 orbital, in contrast, has σ_u symmetry and ionization from this orbital, leading to the $\tilde{\mathbf{B}}\,^2\Sigma_u^+$ state of CO_2^+ (B channel), is enhanced at small alignment angles. When the X channel is suppressed by two-center interference, the X and B channels become comparable in amplitude. Therefore, the structural minimum in channel X provides a natural "window" into lower molecular orbitals, enabling efficient interference of their contributions with that of HOMO. This interference records the ultrafast dynamics in the ion [9]. The use of a long driving wavelength is particularly convenient as it provides sufficient dynamic range in the harmonic spectrum to fully observe this interplay.

A classical calculation of the relation between harmonic photon energy and the time spent by the electron in the continuum helps to illustrate the effect [Fig. 3(a)]. As the position of the dynamical interference is locked to the time spent by the electron in the continuum, an increase in

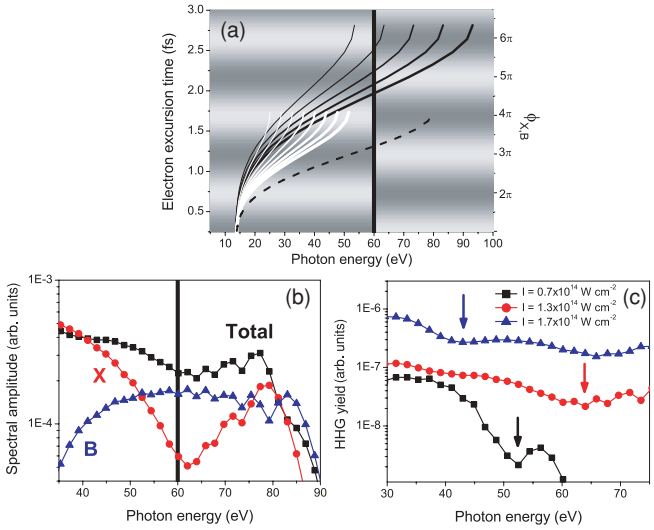

FIG. 3. (Color online) (a) Electron excursion time vs photon energy (short trajectories) calculated classically for CO_2. Black and white solid lines correspond to the conditions of the present work and those of Ref. [9] respectively. Increasing thickness represents increasing intensity $(0.8–1.6) \times 10^{14}$ W cm^{-2} (black) and $(0.6–2.0) \times 10^{14}$ W cm^{-2} (white). The dashed line corresponds to the experiment of Ref. [4], at 3.5×10^{14} W cm^{-2}. The background shading represents the dynamical interference between X and B channels: constructive (light) or destructive (dark). The vertical lines in (a) and (b) show the position of the structural minimum. (b) Calculated harmonic amplitudes in CO_2 with 1300-nm drive field and an intensity of 1.3×10^{14} W cm^{-2} for the X (circles) and B (triangles) channels as well as the total amplitude (squares). (c) Calculated total harmonic yield at three intensities spanning the range used in this work.

the laser intensity causes a shift in the dynamical minima toward higher photon energies, while the structural minimum stays at fixed energy. Thus, a nonmonotonic intensity dependence arises naturally. With increasing intensity, the position of the dynamical minimum in energy passes the window of efficient interference provided by the structural minimum, shifting the overall minimum first below and then above the structural minimum. Once the window of efficient interference is passed, the overall minimum shifts back to the beginning of the window as the next dynamical minimum moves in. Outside the structural window, the contribution of lower orbitals is too weak to produce strong interference.

This interpretation is supported by our calculations for CO_2 aligned with $\Theta = 0^\circ$. The calculation proceeds along the lines of that presented in [9], where the single molecule response is averaged over an alignment distribution of the form $\cos^4\theta$ whose modal value of θ is 30°. The dominant channel at these intensities is the X channel (HOMO). The B channel, although generally of a much smaller amplitude, plays a significant role in the spectral region near the structural minimum when the molecule is parallel to the driving field. The amplitudes from channels X and B interfere, with relative phase going through multiple points of constructive and destructive interference. The time-dependent relative phase ϕ is primarily determined by the energy difference ΔE between the ionic states, evolving as $\phi \approx [(\Delta E)/\hbar]t$, where t is the electron excursion time in the continuum [9,10,26]. The dynamic interference is expected to be destructive if the relative phase ϕ is an odd multiple of π. However, destructive interference flips to a constructive interference above the structural minimum in the channel X (and vice versa for the constructive interference before the minimum) due to the π phase shift of the recombination matrix element for the channel X. Maxima and minima in the dynamic interference shift to higher harmonic numbers with increasing laser intensity [9,10] [Fig. 3(a)], leading to cycling of the dynamical features through the structural window. This cycling results in the shape and position of the overall minimum in the HHG spectrum to be sensitive to intensity, causing it to jump back rather suddenly with increasing intensity [Fig. 3(c)], in qualitative agreement with our measurements.

The extension of electron recollision energies and hence the harmonic spectra, made possible by using a mid-IR driving field, has allowed us to identify the interplay between structural and dynamical interferences in HHG from CO_2. This interplay explains a surprising variation in the position of the minimum observed in the harmonic spectrum of CO_2 at different laser intensities.

Recording broad harmonic spectra across the full region of the structure-related minimum for a range of laser intensities provides a window into recording attosecond multielectron dynamics in many molecules. This opens up a new class of ultrafast experiments where, in a pump-probe scheme, with the pump pulse exciting molecular vibrations [8] (or dissociation), one could use the structural window to record changes in multielectron dynamics caused by the time-dependent coupling between electronic and nuclear degrees of freedom.

The experiment was carried out at the Central Laser Facility (CLF), Rutherford Appleton Laboratory (UK). We thank the CLF staff for the support provided. This work has been funded by Science and Technology Facilities Council (STFC) and Engineering and Physical Sciences Research Council (EPSRC) grants EP/C530764/1, EP/E028063/1, and EP/C530756/2.

[1] M. Lein, N. Hay, R. Velotta, J. P. Marangos, and P. L. Knight, Phys. Rev. Lett. **88**, 183903 (2002).
[2] J. Itatani *et al.*, Nature (London) **432**, 867 (2004).
[3] T. Kanai, S. Minemoto, and H. Sakai, Nature (London) **435**, 470 (2005).
[4] C. Vozzi *et al.*, Phys. Rev. Lett. **95**, 153902 (2005).
[5] J. P. Marangos *et al.*, Phys. Chem. Chem. Phys. **10**, 35 (2008).
[6] S. Baker *et al.*, Science **312**, 424 (2006).
[7] S. Baker *et al.*, Phys. Rev. Lett. **101**, 053901 (2008).
[8] W. Li *et al.*, Science **322**, 1207 (2008).
[9] O. Smirnova *et al.*, Nature (London) **460**, 972 (2009).
[10] O. Smirnova *et al.*, Proc. Nat. Acad. Sci. USA **106**, 16556 (2009).
[11] B. K. McFarland *et al.*, Science **322**, 1232 (2008).
[12] X. X. Zhou, X.-M. Tong, Z. X. Zhao, and C. D. Lin, Phys. Rev. A **71**, 061801(R) (2005).
[13] R. de Nalda *et al.*, Phys. Rev. A **69**, 031804(R) (2004).
[14] B. Shan, S. Ghimire, and Z. Chang, Phys. Rev. A **69**, 021404(R) (2004).
[15] H. Stapelfeldt and T. Seideman, Rev. Mod. Phys. **75**, 543 (2003).
[16] W. Boutu *et al.*, Nature Phys. **4**, 545 (2008).
[17] X. Zhou *et al.*, Phys. Rev. Lett. **100**, 073902 (2008).
[18] S. Patchkovskii, Z. Zhao, T. Brabec, and D. M. Villeneuve, Phys. Rev. Lett. **97**, 123003 (2006).
[19] O. Smirnova *et al.*, Phys. Rev. Lett. **102**, 063601 (2009).
[20] P. Antoine, A. L'Huillier, and M. Lewenstein, Phys. Rev. Lett. **77**, 1234 (1996).
[21] B. L. Henke, E. M. Gullikson, and J. C. Davis, At. Data Nucl. Data Tables **54**, 181 (1993).
[22] F. Rosca-Pruna and M. J. J. Vrakking, Phys. Rev. Lett. **87**, 153902 (2001).
[23] R. Torres, R. de Nalda, and J. P. Marangos, Phys. Rev. A **72**, 023420 (2005).
[24] O. Smirnova, M. Spanner, and M. Ivanov, Phys. Rev. A **77**, 033407 (2008).
[25] R. Velotta, N. Hay, M. B. Mason, M. Castillejo, and J. P. Marangos, Phys. Rev. Lett. **87**, 183901 (2001).
[26] T. Kanai, E. J. Takahashi, Y. Nabekawa, and K. Midorikawa, Phys. Rev. Lett. **98**, 153904 (2007).